Journal of Enzyme Inhibition and Medicinal Chemistry

ISSN: 1475-6366 (Print) 1475-6374 (Online) Journal homepage: http://www.tandfonline.com/loi/ienz20

Metal-based ethanolamine-derived compounds: a note on their synthesis, characterization and bioactivity

Muhammad Amjad, Sajjad H. Sumrra, Muhammad Safwan Akram & Zahid H. Chohan

To cite this article: Muhammad Amjad, Sajjad H. Sumrra, Muhammad Safwan Akram & Zahid H. Chohan (2016): Metal-based ethanolamine-derived compounds: a note on their synthesis, characterization and bioactivity, Journal of Enzyme Inhibition and Medicinal Chemistry, DOI: 10.1080/14756366.2016.1220375

To link to this article: http://dx.doi.org/10.1080/14756366.2016.1220375

Published online: 24 Aug 2016.

Journal of Enzyme Inhibition and Medicinal Chemistry

www.tandfonline.com/ienz
ISSN: 1475-6366 (print), 1475-6374 (electronic)

J Enzyme Inhib Med Chem, Early Online: 1–10
 DOI: 10.1080/14756366.2016.1220375

Taylor & Francis
Taylor & Francis Group

RESEARCH ARTICLE

Metal-based ethanolamine-derived compounds: a note on their synthesis, characterization and bioactivity

Muhammad Amjad[1], Sajjad H. Sumrra[2], Muhammad Safwan Akram[3], and Zahid H. Chohan[4]

[1]*Institute of Chemical Sciences, Bahauddin Zakariya University, Multan, Pakistan,* [2]*Department of Chemistry, Institute of Natural Sciences, University of Gujrat, Gujrat, Pakistan,* [3]*School of Science & Engineering, Teesside University, Middlesbrough, UK, and* [4]*Department of Chemistry, University of Sargodha, Bhakkar Campus, Pakistan*

Abstract

Metal-based ethanolamines, **(L^1)–(L^4)** coordinated with Co(II), Cu(II), Ni(II) and Zn(II) metals in 1:2 (metal:ligand) molar ratio to produce new compounds have been reported. These compounds were screened for their bactericidal/fungicidal activity against a number of bacterial (*Escherichia coli*, *Shigella flexneri*, *Pseudomonas aeruginosa*, *Salmonella typhi*, *Staphylococcus aureus* and *Bacillus subtilis*) and fungal strains (*Trichophyton longifusus, Candida albicans, Aspergillus flavus, Microsporum canis, Fusarium solani* and *Candida glabrata*) alongside against a shrimp species known as *Artemia salina*. The screening results indicated that metal complexes have significantly higher activity than uncomplexed ligands against one or more bacterial/fungal species due to chelation. The ligand (L^4) displayed good bacterial and fungal activity as compared to other ligands. The antibacterial results revealed that the Zn(II) complex **(16)** of (L^4) was found to be the most active complex and Co(II) complex **(14)** of the same ligand (L^4), demonstrated the highest antifungal activity.

Keywords

Antibacterial/antifungal, ethanolamine-derived compounds, metal(II) complexes

History

Received 13 May 2016
Revised 17 July 2016
Accepted 1 August 2016
Published online 22 August 2016

Introduction

Bioactive transition metal complexes have gained increasing interest in metal-based drug chemistry especially as therapeutic agents. Since their discovery in 1864, Schiff's bases have contributed immensely to the development of co-ordination chemistry and acting as an inspiration for the development of novel compounds[1]. The Schiff bases are characterized by an imine group and are formed as a condensation product[2] of primary amine with an aldehyde or ketone in the presence of a dehydrating agent such as $MgSO_4$. A number of Schiff's base metal complexes have displayed bioactivity as antibacterial[3,4], antifungal[5], anticancer[6,7,8], anti-inflammatory[9], anticonvulsant[10], antiviral[11] and analgesic[12] agents. Although metal-based ethanolamines have historically been subjected of many investigations[13,14] due to their use as buffers[15], catalysts[16], inhibitors[17], ion exchangers[18], electroplating and dyes[19], now they are garnering attention for their biological[20] role in plant growth[21] regulation, bacterial and fungal metabolism and as a cytotoxic agent[22]. Metal-based compounds have also been reported to improve electron transfer and efficiency in protein bioelectrochemistry[23,24].

One of the advantages of using Schiff's bases is the ability to control and tune the electronic and steric properties of the ligand attached to the metal. One of the strategies is an appropriate choice of precursor, because that plays a pivotal role by allowing control over nature of donor atoms, number of chelating moieties and the extent of denticity. The new series of ethanolamine-derived compounds **(L^1)–(L^4),** *(E)-2-(((2-hydroxyethyl) imino)methyl)phenol* **(L^1)**, *(E)-2-(((2-hydroxyethyl)imino)methyl)-naphthalen-1-ol* **(L^2)**, *(E)-2-((4-nitrobenzylidene)amino)ethanol* **(L^3)** and *(E)-5-bromo-2-(((2-hydroxyethyl) imino)methyl)phenol* **(L^4)** were synthesized from the reaction of 2-hydroxy-1-naphthaldehyde, 2-hydroxybezaldehyde, 5-bromo-2-hydroxybezaldehyde and 4-nitrobenzaldehyde, respectively, with ethanolamine in equimolar ratio (Scheme 1). The synthesized ligands were further coordinated with Co(II), Cu(II), Ni(II), and Zn(II) metals in 1:2 (metal:ligand) molar ratio to produce new metal complexes (Scheme 2).

The synthesized ligands and their metal(II) complexes have been screened *in vitro* for antibacterial activity against six bacterial species (*Escherichia coli*, *Shigella flexneri*, *Pseudomonas aeruginosa*, *Salmonella typhi*, *Staphylococcus aureus* and *Bacillus subtilis*) and for *in vitro* antifungal activity against six fungal strains (*Trichophyton longifusus*, *Candida albicans, Aspergillus flavus*, *Microsporum canis*, *Fusarium solani* and *Candida glabrata*). Cytotoxicity of the compounds was determined through the help of brine shrimp bioassay.

Materials and methods

All the chemicals used were of analytical grade and were purchased from Sigma Aldrich. Infrared spectra of solid compounds (as KBr disc) were recorded on a Nicolet FT-IR Impact 400D infrared spectrometer. Elemental analysis was carried out on Perkin Elmer and 1H and 13C NMR spectra were recorded on a Bruker Spectrospin Avance DPX-400 spectrometer using TMS as internal standard and d6-DMSO as a solvent. Electron impact mass spectra (EIMS) were recorded on JEOL MSRoute instrument.

Address for correspondence: Zahid H. Chohan, *Department of Chemistry, University of Sargodha, Bhakkar Campus, Pakistan*. E-mail: dr.zahidchohan@gmail.com

Scheme 1. Preparation of ligands.

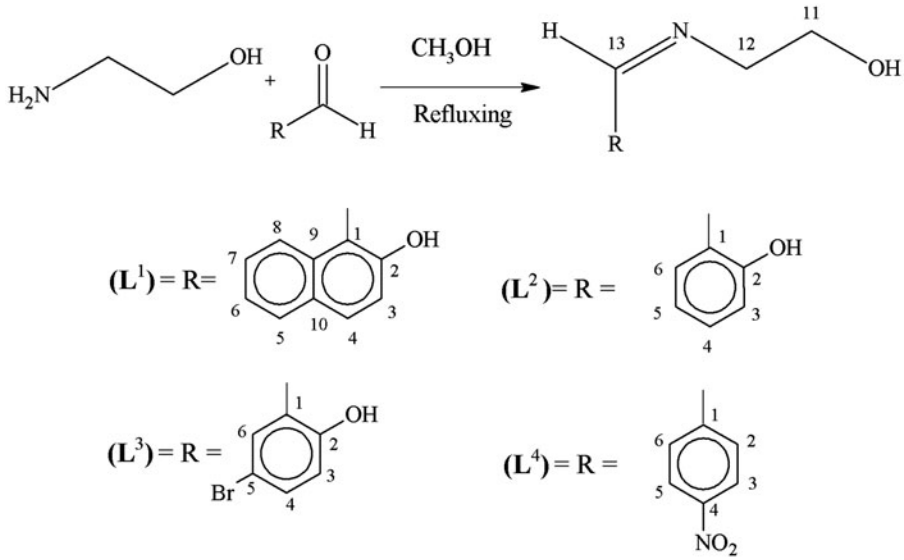

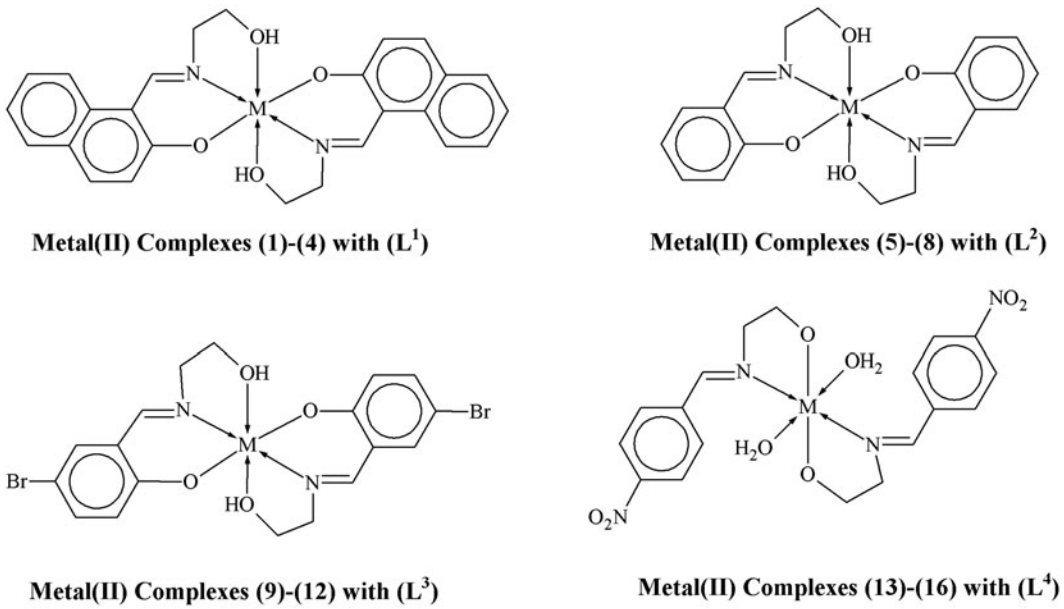

Scheme 2. Metal(II) complexes.

UV-Visible spectra were recorded on ultraviolet spectrometer-1700 (Shimadzu, Japan) in the frequency range of 250–800 nm. Molar conductance of metal complexes was measured using an Inolab Cond 720 Conductivity Bridge at room temperature using 0.001 molar solutions in DMF. A Stanton SM12/S Gouy balance was used to measure the magnetic susceptibility of the metal complexes at room temperature using mercury acetate ligand as a standard. *In vitro* antibacterial, antifungal and cytotoxic properties were studied in collaboration with Research Institute of Chemistry, International Centre for Chemical Sciences, University of Karachi, Pakistan and School of Science and Engineering, Teesside University, UK.

Synthesis of ligands

Different aldehydes such as 2-hydroxy-1-naphthaldehyde, 2-hydroxybezaldehyde, 5-bromo-2-hydroxybezaldehyde and 4-nitrobenzaldehyde were individually dissolved in ethanol (25 mL) and added respectively to a refluxed solution of ethanolamine in ethanol (10 mL) in an equimolar ratio. The reaction mixture was refluxed for 3 h and consequently precipitated while being monitored. The solid product thus obtained was filtered, washed with ethanol and dried. It was re-crystallized in hot ethanol/methanol (1:1). The same method was used for the preparation of all other ligands (**L^1**)–(**L^4**).

(E)-2-(((2-hydroxyethyl)imino)methyl)naphthalen-1-ol (**L^1**)

Yield: (1.64 g, 76%); mp 151 °C; color (dark yellow); IR (KBr, cm^{-1}): 3438 (aryl-OH), 3385(alc-OH), 1627 (–HC=N), 1603 (C–H) and 1584 (C=C); ^{1}H NMR (ppm d_6-DMSO): δ 3.65 (s, 1H, alc-OH), 4.50 (*t*, 2H, C_{12}–H), 5.85 (*t*, 2H, C_{11}–H), 7.15 (d, 1H, $J = 9.0$ Hz, C_3–H), 7.41 (*t*, 1H, $J = 7.4$ Hz, C_6–H), 7.53 (*t*, 1H, $J = 7.4$ Hz, C_7–H), 7.80 (d, 1H, $J = 7.8$ Hz, C_4–H), 7.95 (d, 1H,

$J = 9.0$ Hz, C_5–H), 8.22 (d, 1H, $J = 8.5$ Hz, C_8–H), 8.53 (s, 1H, C_{13}–H), 9.88 (s, 1H, aryl-OH); 13C NMR (DMSO-d_6): δ 59.3 (C_{11}), 69.5 (C_{12}), 116.4 (C_1), 122.1 (C_6), 125.5 (C_3), 126.2 (C_8), 126.9 (C_{10}), 127.7 (C_7), 128.9 (C_5), 134.3 (C_9), 136.4 (C_4), 159.6 (C_2), 162.8 (C_{13}); Mass Spectrum (ESI): $[M]^+ = 215.25$. UV-Visible: 27 335 and 31 284 cm^{-1}. Anal. Calc. for $C_{13}H_{13}NO_2$ (215.25) C, 72.54; H, 6.09; N, 6.51; O, 14.87 and found C, 72.48; H 6.04; O, 14.83.

(E)-2-(((2-hydroxyethyl)imino)methyl)phenol[25] (L^2)

Yield (1.22 g, 74%); mp 92 °C; color (yellow); IR (KBr, cm^{-1}): 3450 (aryl-OH), 3380(alc-OH),1625 (–HC=N) and 1596 (C=C); ^{1}H NMR (ppm d_6-DMSO): δ 3.63 (s, 1H, alc-OH),4.50 (*t*, 2H, C_{12}-H), 5.85 (*t*, 2H, C_{11}–H), 7.0 (*t*, 1H, $J = 8.5$ Hz, C_4–H), 7.11 (d, 1H, $J = 7.9$ Hz, C_6–H), 7.45 (*t*, 1H, $J = 7.5$ Hz, C_5–H), 7.69 (d, 1H, $J = 7.8$ Hz, C_3–H), 8.50 (s, 1H, C_{13}–H), 9.91(s, 1H, aryl-OH); 13C NMR (DMSO-d_6): δ 59.4 (C_{11}), 69.7 (C_{12}), 117.5 (C_3), 119.3 (C_1), 121.7(C_5), 131.1 (C_6), 133.6 (C_4), 159.9 (C_2), 162.5 (C_{13}); Mass Spectrum (ESI): $[M]^+ = 165.19$. UV-Visible: 27 233 and 31 050 cm^{-1}. Anal. calcd. for $C_9H_{11}NO_2$ (465.19): C, 65.44; H, 6.71; N, 8.48; O, 19.37. Found: C, 65.38; H, 6.67; N, 19.33.

(E)-4-Bromo-2-(((2-hydroxyethyl)imino)methyl)phenol (L^3)

Yield (1.51 g, 78%); mp: 99 °C, color (orange yellow); IR (KBr, cm^{-1}): 3453 (aryl-OH), 3382(alc-OH), 1622 (–HC=N) and 1590 (C=C); ^{1}H NMR (ppm d_6-DMSO): δ 3.67 (s, 1H, alc-OH),4.50 (*t*, 2H, C_{12}–H), 5.85 (*t*, 2H, C_{11}–H), 7.12 (d, 1H, $J = 8.7$ Hz, C_3–H), 7.50 (dd, 1H, $J = 8.7$, 2.5 Hz, C_5–H), 8.10 (d, 1H, $J = 2.5$ Hz, C_6–H), 8.57 (s, 1H, C_{13}–H), 9.93 (s, 1H, aryl-OH); ^{13}C NMR (DMSO-d_6): δ 58.9 (C_{11}), 68.1 (C_{12}), 118.7 (C_3), 122.5 (C_1), 125.2 (C_5), 127.7 (C_4), 133.1(C_6), 159.2 (C_2), 161.9 (C_{13}); mass spectrum (ESI): $[M]^+ = 165.19$. UV-Visible: 27 461 and 31 338 cm^{-1}. Anal. calcd. for$C_9H_{10}BrNO_2$ (244.1): C, 44.29; H, 4.13; Br, 32.74; N, 5.74. Found: C, 44.23; H, 4.11; Br,32.68; N, 5.70.

(E)-2-((4-nitrobenzylidene)amino)ethanol[25] (L^4)

Yield (1.55 g, 80%); mp: 88 °C, color (reddish brown); IR (KBr, cm^{-1}): 3460 (aryl-OH), 3390(alc-OH), 1632 (–HC=N), 1595 (C=C) and 1424 (NO_2); ^{1}H NMR (ppm d_6-DMSO): δ 3.69 (s, 1H, alc-OH), 4.50 (*t*, 2H, C_{12}–H), 5.85 (*t*, 2H, C_{11}–H), 8.10 (dd, 2H, $J = 8.7$, 2.5 Hz, C_2–H and C_6–H), 8.33 (dd, 2H, $J = 8.7$, 2.5 Hz, C_3–H and C_5–H), 8.65 (s, 1H, C_{13}–H); 13C NMR (DMSO-d_6): δ 59.3 (C_{11}), 68.6 (C_{12}), 120.6 (C_3), 122.4 (C_5), 130.5 (C_1), 131.0 (C_6), 152.3

(C_4), 158.8(C_2), 162.2 (C_{13}); mass spectrum (ESI): $[M]^+ = 194.19$. UV-Visible: 27 590 and 31 410 cm^{-1}. Anal. calcd. for $C_9H_{10}N_2O_3$ (194.19): C, 55.67; H, 5.19; N, 14.44. Found: C, 55.62; H, 5.16; N, 14.11.

Synthesis of the transition metal(II) complexes

All complexes were prepared according to the standard procedure in which a methanol solution (20 mL) of the respective metal(II) as a chloride (5 mmol) was added to a refluxed methanol solution (30 mL) of the ligand (10 mmol). The mixture was further refluxed for 3 h leading to a precipitated product. It was then cooled to room temperature, filtered, washed with methanol and finally with diethyl ether. The precipitated product thus obtained was dried and recrystallized in a mixture of hot aqueous methanol:ethanol (1:2) to obtain TLC pure product.

NMR data of the Zn(II) complexes

$[Zn(L^1)_2]$ **(4):** ^{1}H NMR (DMSO-d_6, δ, ppm): 3.78 (s, 1H, alc-OH), 4.61 (*t*, 2H, C_{12}–H), 5.91 (*t*, 2H, C_{11}–H), 7.26 (d, 1H, C_3–H), 7.46 (*t*, 1H, C_6–H), 7.59 (*t*, 1H, C_7–H), 7.90 (d, 1H, C_4–H), 7.99(d, 1H, C_5–H), 8.26 (d, 1H, C_8–H), 8.64 (s, 1H, C_{13}–H); 13C NMR (DMSO-d_6, δ, ppm): 60.1(C_{11}), 70.3 (C_{12}), 117.5 (C_1), 129.1 (C_6), 125.5 (C_3), 126.7 (C_8), 127.5 (C_{10}), 128.2 (C_7), 129.6(C_5), 135.0 (C_9), 136.4 (C_4), 160.6 (C_2), 163.9 (C_{13}).

$[Zn(L^2)_2]$ **(8):** ^{1}H NMR (DMSO-d_6, δ, ppm): 3.79 (s, 1H, alc-OH), 4.62 (*t*, 2H, C_{12}–H),5.94 (*t*, 2H, C_{11}–H), 7.07 (*t*, 1H, C_4–H), 7.18 (d, 1H, C_6–H), 7.51 (*t*, 1H, C_5–H), 7.79 (d, 1H, C_3–H), 8.63 (s, 1H, C_{13}–H); 13C NMR (DMSO-d_6, δ, ppm): δ 60.4 (C_{11}), 70.7 (C_{12}), 117.5 (C_3), 119.3 (C_1), 123.3 (C_5), 131.1 (C_6), 134.2 (C_4), 161.0 (C_2), 163.6 (C_{13}).

$[Zn(L^3)_2]$ **(12):** ^{1}H NMR (DMSO-d_6, δ, ppm): 3.70 (s, 1H, alc-OH), 4.60 (*t*, 2H, C_{12}–H), 5.95 (*t*, 2H, C_{11}–H), 7.23 (d, 1H, C_3–H), 7.55 (dd, 1H, C_5–H), 8.19 (d, 1H, C_6–H), 8.61 (s, 1H, C_{13}–H);^{13}C NMR (DMSO-d_6, δ, ppm): δ 59.8 (C_{11}), 69.1 (C_{12}), 118.7 (C_3), 123.5 (C_1), 125.7 (C_5), 128.3(C_4), 133.8 (C_6), 160.2 (C_2), 163.0 (C_{13}).

$[Zn(L^4)_2]$ **(16):** ^{1}H NMR (DMSO-d_6, δ, ppm): 4.59 (*t*, 2H, C_{12}–H), 5.93 (*t*, 2H, C_{11}–H), 8.18(dd, 2H, C_2–H and C_6–H), 8.39 (dd, 2H, C_3–H and C_5–H), 8.62 (s, 1H, C_{13}–H), 10.3 (s, 4H, H_2O); 13C NMR (DMSO-d_6, δ, ppm): δ 60.2 (C_{11}), 69.7 (C_{12}), 121.4 (C_3), 122.9 (C_5), 131.5 (C_1), 131.8 (C_6), 152.9 (C_4), 159.7 (C_2), 163.3 (C_{13}).

Biological activity

Antibacterial activity (*in vitro*)

All the newly synthesized ethanolamine-derived compounds **(L^1)–(L^4)** and their metal(II) complexes **(1)–(16)** were screened *in vitro* for their antibacterial activity against four Gram-negative (*E. coli*, *S. flexneri*, *P. aeruginosa*, *S. typhi*) and two Gram-positive (*S. aureus*, *B. subtilis*) bacterial strains by agar-well diffusion method[26]. The wells (6 mm in diameter) were dug in the media with the help of a sterile metallic borer with centers of at least 24 mm apart. Two to eight hours old bacterial inocula containing approximately 104–106 colony-forming units (CFU/mL) were spread on the surface of the nutrient agar with the help of a sterile cotton swab. The recommended concentration of the test sample (1 mg/mL in DMSO) was introduced in the respective wells. Other wells supplemented with DMSO and reference antibacterial drug (imipenum) served as a negative and positive control, respectively. The plates were incubated at 37 °C for 24 h. Activity was determined by measuring the diameter of clear zones showing complete inhibition (mm). In order to confirm the effect of DMSO in the biological screening, alternate studies on DMSO solution showed no activity against any bacterial strains.

Antifungal activity (*in vitro*)

Antifungal activity was studied against six fungal strains (*T. longifusus*, *C. albican*, *A. flavus*, *M. canis*, *F. solani* and *C. glabrata*). Sabouraud dextrose agar (Oxoid, Hampshire, England) was seeded with 10^5 (cfu) mL^{-1} fungal spore suspensions and transferred to petri plates. Discs soaked in 20 mL (200 µg/mL in DMSO) of the compounds were placed at different positions on the agar surface. The plates were incubated at 32 °C for 7 days. The results were recorded as percentage of inhibition and compared with the standard drugs miconazole and amphotericin B.

Minimum inhibitory concentration (MIC)

Compounds containing promising antibacterial activity were selected for minimum inhibitory concentration (MIC) studies. The MIC was determined using the disc diffusion technique[27] by preparing discs containing diluted samples at 10, 25, 50, and

Table 1. Physical measurements and analytical data of metal (II) complexes (**1**)–(**16**).

No	Structure	Yield (%)	MW/Formula	M.P (°C)	Elemental analysis (%) Calc (Found) C	H	N	M
1	$[Co(L^1–H)_2]$	70	[487.41] $C_{26}H_{24}N_2O_4Co$	166–168	64.07(64.01)	4.96 (4.92)	5.75 (5.72)	12.09 (12.04)
2	$[Ni(L^1–H)_2]$	70	[487.17] $C_{26}H_{24}N_2O_4Ni$	220–222	64.10 (64.01)	4.97 (4.92)	5.75 (5.71)	12.05 (12.01)
3	$[Cu(L^1–H)_2]$	75	[492.02] $C_{26}H_{24}N_2O_4Cu$	185–187	64.77 (64.71)	4.92 (4.89)	5.69 (5.65)	12.92 (12.88)
4	$[Zn(L^1–H)_2]$	83	[493.89] $C_{26}H_{24}N_2O_4Zn$	197–199	63.23 (63.18)	4.90 (4.86)	5.67 (5.62)	13.24 (13.20)
5	$[Co(L^2–H)_2]$	71	[387.30] $C_{18}H_{20}N_2O_4Co$	175–176	55.82 (55.77)	5.21 (5.18)	7.23 (7.20)	15.22 (15.18)
6	$[Ni(L^2–H)_2]$	74	[387.06] $C_{18}H_{20}N_2O_4Ni$	230–232	55.86 (55.80)	5.21 (5.17)	7.24 (7.20)	15.16 (15.12)
7	$[Cu(L^2–H)_2]$	81	[391.91] $C_{18}H_{20}N_2O_4Cu$	194–196	55.16 (55.11)	5.14 (5.10)	7.15 (7.12)	16.21 (16.17)
8	$[Zn(L^2–H)_2]$	82	[393.77] $C_{18}H_{20}N_2O_4Zn$	270–272	54.90 (54.85)	5.12 (5.09)	7.11 (7.06)	16.61 (16.56)
9	$[Co(L^3–H)_2]$	85	[545.09] $C_{18}H_{18}Br_2N_2O_4Co$	225–227	39.66 (39.61)	3.33 (3.29)	5.14 (5.11)	10.81 (10.77)
10	$[Ni(L^3–H)_2]$	80	[544.85] $C_{18}H_{18}Br_2N_2O_4Ni$	194–196	39.68 (39.64)	3.33 (3.29)	5.14 (5.10)	10.77 (10.73)
11	$[Cu(L^3–H)_2]$	84	[549.70] $C_{18}H_{18}Br_2N_2O_4Cu$	214–216	39.33 (39.29)	3.30 (3.27)	5.10 (5.07)	11.56 (11.52)
12	$[Zn(L^3–H)_2]$	80	[551.56] $C_{18}H_{18}Br_2N_2O_4Zn$	211–212	39.20 (39.15)	3.29 (3.26)	5.08 (5.04)	11.86 (11.82)
13	$[Co(L^4)_2]$	74	[481.32] $C_{18}H_{22}N_4O_8Co$	176–177	44.92 (44.87)	4.61 (4.57)	11.64 (11.60)	12.24 (12.20)
14	$[Ni(L^4)_2]$	82	[481.07] $C_{18}H_{22}N_4O_8Ni$	206–208	44.94 (44.89)	4.61 (4.58)	11.65 (11.60)	12.20 (12.16)
15	$[Cu(L^4)_2]$	77	[485.84] $C_{18}H_{22}N_4O_8Cu$	190–191	44.49 (44.44)	4.56 (4.53)	11.53 (11.50)	13.08 (13.05)
16	$[Zn(L^4)_2]$	78	[487.80] $C_{18}H_{22}N_4O_8Zn$	278–280	44.32 (44.27)	4.55 (4.51)	11.49 (11.45)	13.41 (13.37)

100 g mL^{-1} concentrations of the compounds along with standards at the same concentrations.

Cytotoxicity (*in vitro*)

Brine shrimp assay was done using the protocol of Meyer et al.[28], the details of which are reproduced here. Brine shrimp (Artemia salina leach) eggs were hatched in a shallow rectangular plastic dish (22 × 32 cm), filled with artificial seawater prepared from commercial salt mixture and double-distilled water. An unequal partition was made in the plastic dish with the help of a perforated device where approximately 50 mg of eggs were sprinkled into the darkened larger compartment while smaller matter compartment was exposed to the ordinary light. After two days, nauplii were collected from the unsheltered side. A sample of the test compound was prepared by dissolving 20 mg of each compound in 2 mL of DMF. From this stock solutions 5, 50 and 500 µg/mL were transferred to nine vials (three for each dilutions were used for each test sample and LD_{50} was calculated as the mean of these three values) and one vial was kept as control having 2 mL of DMF only. The solvent was allowed to evaporate overnight. After two days, when shrimp larvae were ready, 1 mL of seawater and 10 shrimps were added to each vial (30 shrimps/dilution) and the volume was adjusted with seawater to 5 mL per vial[28]. After 24 h the number of survivors was counted. Data were analyzed by a computer program to determine the LD_{50} values[29].

Results and discussion

The condensation reaction of ethanolamine with 2-hydroxy-1-naphthaldehyde/2-hydroxy benzaldehyde/5-bromo-2-hydroxybenzaldehyde/4-nitrobenzaldehyde in an equimolar ratio afforded four ligands (**L^1**)–(**L^4**) (Scheme 1). These colored ligands were stable in both air and moisture. These microcrystalline solids melted at 88–151 °C and were soluble in DMSO and DMF at room temperature and in methanol and ethanol on heating. The ligands (**L^1**)–(**L^3**) were found to be tridentate and the ligand (**L^4**) to be bidentate which reacted readily with Co(II), Cu(II), Ni(II) and Zn(II) metals as their chlorides in methanol to form their metal(II) complexes (Scheme 2).

All the synthesized metal(II) complexes were microcrystalline and had an intense color except Zn(II) complexes, which were off-white. The metal(II) complexes decomposed (Table 1) without melting and were insoluble in common organic solvents such as ethanol, methanol, dichloromethane and acetone but soluble in DMSO and DMF. The spectral data and elemental analysis of the prepared ligands and their metal(II) complexes were in a good agreement with their proposed structures, indicating the high purity of all the compounds. The analytical data of the complexes indicated a 1:2 metal: ligand stoichiometry.

IR spectra

The significant and distinctive IR spectral bands are reported in the experimental part and in Table 2. All Schiff's base ligands possessed potentially active donor sites capable of coordinating with metal atoms such as azomethine nitrogen (–HC=N), aliphatic and aromatic hydroxyl (–OH) groups. The Schiff bases (**L^1**)–(**L^4**) possessed the characteristic azomethine (–HC=N) stretching[30] at 1622–1632 cm^{-1} giving a clue of condensation product. All the ligands (**L^1**)–(**L^4**) displayed aliphatic hydroxyl (–OH) stretching at 3380–3390 cm^{-1}, however, ligands (**L^1**)–(**L^3**) additionally showed aromatic hydroxyl (–OH) stretching[31] at 3438–3390 cm^{-1}. The ligand (**L^4**) showed a band at 1424 cm^{-1}

Table 2. Conductivity, magnetic and spectral data of metal(II) complexes (**1**)–(**16**).

No	Ω_M (Ω^{-1} cm^2 mol^{-1})	B.M μ_{eff}	λ_m (cm^{-1})	IR (cm^{-1})
1	15.9	4.35	8723, 17 690, 29 820	3370 (OH), 1616 (HC = N), 1370 (C–O), 520 (M–N), 442 (M–O)
2	15.7	3.56	8635, 17 717, 25 817, 29 781	3372 (OH), 1615 (HC = N), 1372 (C–O), 535 (M–N), 450 (M–O)
3	14.6	1.66	8897, 17 783, 29 816	3371 (OH), 1620 (HC = N), 1373 (C–O), 529 (M–N), 448 (M–O)
4	14.9	Dia	28 915	3373 (OH), 1618 (HC = N), 1371 (C–O), 533 (M–N), 450 (M–O)
5	16.2	4.53	8650, 17 729, 29 841	3366 (OH), 1612 (HC = N), 1372 (C–O), 522 (M–N), 446 (M–O)
6	15.8	3.41	8712, 17 761, 25 778, 29 738	3365 (OH), 1610 (HC = N), 1370 (C–O), 536 (M–N), 445 (M–O)
7	15.6	1.71	8937, 17 892, 29 812	3365 (OH), 1615 (HC = N), 1371 (C–O), 526 (M–N), 443 (M–O)
8	15.1	Dia	28 928	3368 (OH), 1613 (HC = N), 1373 (C–O), 532 (M–N), 440 (M–O)
9	16.2	4.38	8680, 17 523, 29 831	3368 (OH), 1611 (HC = N), 1377 (C–O), 540 (M–N), 449 (M-–O)
10	15.2	3.48	8786, 17 777, 25 719, 29 781	3367 (OH), 1610 (HC = N), 1376 (C–O), 524 (M–N), 453 (M–O)
11	16.0	1.74	8727, 17 765, 29 788	3370 (OH), 1612 (HC = N), 1375 (C–O), 536 (M–N), 448 (M–O)
12	15.0	Dia	28 841	3377 (OH), 1608 (HC = N), 1377 (C–O), 528 (M–N), 451 (M–O)
13	14.6	4.45	8790, 17 800, 29 805	3470 (H_2O), 1620 (HC = N), 540 (M–N), 455 (M–O)
14	16.5	3.51	8696, 17 871, 25 719, 29 778	3471 (H_2O), 1622 (HC = N), 544 (M–N), 459 (M–O)
15	15.4	1.70	8866, 17 857, 29 858	3470 (H_2O), 1623 (HC = N), 541 (M–N), 460 (M–O)
16	15.1	Dia	28 932	3473 (H_2O), 1619 (HC = N), 543 (M–N), 463 (M–O)

resulting from NO_2 vibrations. The comparison of the IR spectra of the Schiff's bases **(L^1)–(L^4)** with their metal(II) complexes **(1)–(16)** indicated that the Schiff bases were principally coordinated to the metal(II) atoms in a bi- and tridentate fashion. The vibrations of azomethine-N group present in all the metal complexes (**1**)–(**16**) and aliphatic-O appearing in the spectra of metal(II) complexes **(1)–(12)** shifted to lower frequency (07–15 cm^{-1}) at 1608–1623 and 3365–3377 cm^{-1}, respectively, representing the mode of coordination of the azomethine nitrogen[32] and hydroxyl-O with the metal(II) atoms. Absence of bands at 3438–3490 and 3380–3390 cm^{-1} due to aliphatic and aromatic ν(OH) and consequent appearance of a new band[33] at 1370–1377 cm^{-1} attributed to ν (C–O) in the metal(II) complexes **(1)–(16)**, confirmed the deprotonation and coordination of aromatic and aliphatic ν (OH) to the metal(II) atoms. The following observations further support the mode of chelation:

- Appearance of the new bands at 520–543 and 440–460 cm^{-1} could be assigned to ν(M–O) and ν(M–N) vibrations[34] in the metal complexes which are absent in ligands.
- The metal(II) complexes **(13)–(16)** demonstrated[35] new broad bands at 3468–3478 cm^{-1} which can likely be attributed to water molecules coordinated to the metal atoms. These bands were only observed in the spectra of the metal complexes.

These clues supported the evidence of the participation of azomethine-N and deprotonation/coordination of hydroxyl-O with the metal(II) ions.

^{1}H NMR spectra

^{1}H NMR spectra of the ligands (**L^1**)–(**L^4**) and their diamagnetic Zn(II) complexes were recorded in DMSO-d_6 and the details are provided in the experimental section. ^{1}H NMR spectradisplayed[36] characteristic azomethine (–HC=N) protons at 8.53–8.65 ppm as a singlet providing a strong evidence for the condensation of amino group of the ethanolamine with aldehydes. All of the ligands (**L^1**)–(**L^4**) displayed aliphatic (–OH) proton at 5.63–5.99 ppm as a singlet and C_{11}–H and C_{12}–H protons at 4.50 and 5.85 ppm as triplet, respectively. The ligands (**L^1**)–(**L^3**) possessed aromatic (–OH) proton at 9.88–9.93 ppm. Ligand (**L^1**) displayed other C_{3-5}–H and C_8–H protons as a double of doublet at 7.15–8.22 ppm, respectively, but C_6–H and C_7–H protons appeared as a triplet at 7.41 and 7.53 ppm, respectively. Similarly, the ligand (**L^2**) exhibited C_4–H and C_5–H protons at 7.0 and 7.45 ppm as triplet and, C_3–H and C_6–H protons as a doublet at 7.11 and 7.69 ppm, respectively. The C_3–H and C_6–H protons of ligand (**L^3**) were found at 7.12 and 8.10 ppm as a doublet and C_5–H proton observed at 7.50 ppm as a double of doublet. ^{1}H NMR spectra of the ligand (**L^4**) showed the C_2–H, C_6–H and, C_3–H and C_5–H protons at 8.10 and 8.33 ppm as double of doublet. The disappearance of hydroxyl proton at 9.88–9.93 ppm in the spectra of Zn(II) complexes confirmed deprotonation and coordination of the hydroxyl-O with the metal atom. The coordination of the azomethine-N was evident by downfield shifting of all the proton signals in their Zn(II) complexes. A strong singlet was observed at 10.3 ppm in the Zn(II) complex **(16)** due to the coordination of water molecule with the Zn(II) metal atom. All protons underwent downfield shift by 0.05–0.12 ppm due to the increased conjugation on coordination with the zinc metal atom. The number of protons calculated from the integration curves[34] and obtained values of the expected CHN analysis agreed well with each other.

^{13}C NMR spectra

The ^{13}C-NMR spectra of the Schiff bases and their diamagnetic Zn(II) complexes were recorded in DMSO-d_6 and are reported along with their possible assignments in the experimental section and all the carbon atoms were found in the expected region. The ^{13}C-NMR spectra of the Schiff base ligands **(L^1)–(L^4)** displayed distinctive and representative (C_{11}, C_{12}) carbons of ethylene group and (C_{13}) carbons of azomethine (–HC=N) at 58.9–69.7 and 161.9–162.8 ppm, respectively. The remaining other (C_1)–(C_{10}) carbons of aromatic rings were observed at 116.4–159.9 ppm. Downfield shifting of the azomethine carbons found in the uncomplexed Schiff bases from161.9–162.8 ppm to 163.0–163.9 ppm in their Zn(II) complexes was due to shifting of electronic density toward the Zn(II) ion. Similarly, all carbons of methylene groups and aromatic rings being near to the coordination sites also showed downfield shifting by 0.5–1.1 ppm due to the increased conjugation and coordination with the metal atoms. The downfield shifting also confirmed the coordination of the azomethine to the zinc metal atom. Moreover, the presence of the number of carbons is well in agreement with the expected values[37]. Furthermore, the conclusions drawn from these studies present further support to the modes of bonding discussed in their IR and ^{1}H NMR spectra.

Mass spectra

The mass fragmentation pattern of the ligands (**L^1**)–(**L^3**) followed the cleavage of C=N (exocyclic) and C=C bonds. The mass spectral data and the stable fragmentation values of the ligands have already been detailed in the experimental section. All the

ligands showed pronounced molecular ion peaks. The data of the Schiff bases shown by mass spectra strongly confirmed the formation of the ligands possessing proposed structures and also, their bonding pattern.

Molar conductances and magnetic measurements

Molar conductance studies of the metal(II) complexes **(1)–(16)** were carried out in DMF and their molar conductance data (14.6–16.9 ohm^{-1} cm^2 mol^{-1}) showed (Table 1) that these complexes were non electrolytic[38] in nature. The magnetic moment (B.M) values of all the metal(II) complexes **(1)–(16)** were measured at room temperature. The observed magnetic moment value of Co(II)complexes were found in the range of 4.35–4.53 B.M indicating that Co(II) complexes as a high-spin with potentially three unpaired electrons in an octahedral environment[39]. The Ni(II) complexes displayed magnetic moment values in the range of 3.41–3.56 B.M indicative of two unpaired electrons per Ni(II) ion suggesting these complexes to have an octahedral[40] geometry. The measured magnetic moment values 1.66–1.74 B.M for Cu(II) complexes are indicative of one unpaired electron per Cu(II) ion for d^9-system suggesting octahedral[41] geometry. All the Zn(II) complexes were found to be diamagnetic[42] as expected.

Electronic spectra

The UV-Visible spectra of all the ligands demonstrated two bands at 27 233–27 590 cm^{-1} and 31 050–31 410 cm^{-1}, respectively. The first band appeared due to n–π^* transition of –C=N group, while the second band would be assigned to π–π^* transition of the phenyl group. After complexation, n–π^* transition of ligand shifted to a higher wavelength which revealed the coordination of ligand with metallic ions[43,44]. The electronic spectra of Co(II) complexes generally showed[45] three absorption bands in the region 8650–8790, 17 523–17 800 and 29 805–29 841 cm^{-1} which may be assigned to $4T_1g \rightarrow 4T_2g(F)$, $4T_1g \rightarrow 4A_2g(F)$ and $4T_1g \rightarrow 4Tg(P)$ transitions respectively, and are suggestive of octahedral geometry around the Co(II) ion. The electronic spectral data of Ni(II) complexes showed[46] the bands in the region 8635–8786, 17 717–17 871 and 25 719–25 717 cm^{-1} assigned, respectively, to the d–d transitions of $3A_2g(F) \rightarrow 3T_2g(F)$ and $3A_2g(F) \rightarrow 3T_1g(F)$. Also, a strong band due to metal to ligand charge transfer was appeared at 29 738–29 781 cm^{-1}. The electronic spectra of all the Cu(II) complexes exhibited[47] absorption bands in the region at 8727–8937 and 17 765–17 892 cm^{-1} which may be assigned to the transitions $2Eg \rightarrow 2T_2g$. The high energy band at 29 788–29 858 cm^{-1} was due to forbidden ligand to metal charge transfer. On the basis of electronic spectra, octahedral geometry around the Cu(II) ion was suggested. The Zn(II) complexes did not show any d–d transition thus showing diamagnetic nature and their spectra were dominated only by a charge transfer band[48] at 28 841–28 932 cm^{-1}.

Biological screening

*Antibacterial bioassay (*in vitro*)*

The newly produced Schiff's bases **(L^1)–(L^4)** and their metal(II) complexes **(1)–(16)** were screened for their *in vitro* antibacterial activity against *E. coli*, *S. flexneri*, *P. aeruginosa*, *S. typhi*, *S. aureus* and *B. subtilis* bacterial strains according to the standard procedures[26] and results are reported in Table 3. The obtained results were compared with those of the standardized drug sample of imipenum (Figure 1). The synthesized ligand (**L^1**) displayed a weaker (07–08 mm clearance zone (cz) or zone of inhibition) activity against *E. coli* and *B. subtilis* and the remaining strains displayed moderate (10–13 mm) activity. Ligand (**L^2**) presented a weaker (8 mm) activity against *S. typhi* and the remaining strains showed moderate (9–13 mm) activity. Ligand (**L^3**) demonstrated moderate (11–12 mm) activity against *S. flexneri*, *P. aeruginosa* and *B. subtilis* and, other remaining strains observed significant (16–17 mm) activity. The ligand (**L^4**) experienced overall significant (15–17 mm) activity. The metal complex (**1**) showed moderate (14 mm) activity against *E. coli* and *B. subtilis* and other remaining strains experienced significant (15–19 mm)

Table 3. Antibacterial bioassay of ligands (**L^1**)–(**L^4**) and metal(II) complexes **(1)–(16)**.

	[Zone of inhibition (mm)]							
	Gram-negative				Gram-positive			
Compounds	(a)	(b)	(c)	(d)	(e)	(f)	(SA)	Average
L^1	08	13	11	10	13	07	2.50	10.33
L^2	13	11	12	08	09	11	1.86	10.67
L^3	16	12	11	17	16	12	2.61	14.00
L^4	16	17	15	17	16	15	0.89	16.00
1	14	19	17	15	19	14	2.59	16.50
2	17	18	12	17	18	14	2.45	16.00
3	16	17	18	13	16	12	2.34	15.33
4	13	16	19	16	20	15	2.59	16.50
5	18	17	19	14	12	18	2.73	16.33
6	16	18	16	13	14	16	1.76	15.50
7	17	19	15	16	16	16	1.38	16.50
8	20	17	19	15	16	17	2.50	17.67
9	20	21	17	22	22	18	2.10	20.00
10	22	16	19	19	23	21	2.53	20.00
11	20	17	16	21	19	20	1.94	18.83
12	18	24	19	23	20	21	2.32	20.83
13	21	23	16	20	19	18	2.58	19.67
14	20	17	21	22	24	22	2.37	21.00
15	19	22	17	19	25	20	2.80	20.33
16	22	21	22	24	21	21	1.17	21.83
SD	25	26	25	27	27	28	1.17	25.83

Average activity of ligand (**L^1**)–(**L^4**) = 12.75 mm; Average activity of complexes **(1)–(16)** = 18.74 mm; (a) *E. coli* (b) *S. flexneri* (c) *P. aeruginosa* (d) *S. typhi* (e) *S. aureus* (f) *B. subtilis*; SD: standard drug (Imipenum); weaker = 0–08 mm, moderate = 09–14 mm, above 14 mm = significant, SA: statistical analysis.

activity. Complex (**2**) showed moderate (12–14 mm) activity against *P. aeruginosa* and *B. subtilis* and left behind strains practiced significant (17–18 mm) activity. Compound (**3**) exhibited moderate (12–13 mm) activity against *S. typhi* and *B. subtilis* and, left over demonstrated significant (16–18 mm) activity. Beside this, the compound (**4**) revealed significant (15–20 mm) activity against all bacterial strains except *E. coli* which observed moderate (13 mm) activity. Also, the complexes **(5)** and **(6)** displayed moderate (12–14 mm) activity against *Salmonella typhi* and *Staphylococcus aureus* and, remaining strains revealed significant (17–19 mm) activity. However, the complexes (**7**)–(**16**) displayed overall significant (15–25 mm) activity against all bacterial strains. The data reported in Table 3 clearly indicates that ($\mathbf{L^4}$) exhibited overall good bacterial activity as compared to other three ligands. The Zn(II) complex (**16**) of ($\mathbf{L^4}$) were found to be the most active complexes. The metal(II) complexes showed[40] higher activity results upon complexation rather than their uncomplexed Schiff's bases.

Antifungal bioassay (in-vitro)

The antifungal screening of all the synthesized compounds was carried out against *T. longifusus, C. albicans, A. flavus, M. canis, F. solani* and *C. glabrata* fungal strains (Table 4) according to the literature protocol[23]. The results of inhibition were compared with the results of standard drugs, miconazole and amphotericin B (Figure 2). Ligand ($\mathbf{L^1}$) exhibited significant (55%) activity against *A. flavus* fungal strain, moderate (37–45%) activity against *T. longifusus*, *M. canis* and *C. glabrata* and weaker (17%) activity against *C. albicans* and but inactive against *F. solani* begging further investigation why that may be? Similarly, the ligand ($\mathbf{L^2}$) possessed significant (56%) activity against *C. albicans* and moderate (38–49%) activity against *T. longifusus, A. flavus, F. solani*, weaker (30%) activity against *C. glabrata* but no activity was observed in *A. flavus.* However, the compound ($\mathbf{L^3}$) and ($\mathbf{L^4}$) displayed overall significant (55–63%) activity against all fungal strains. The complex (**1**) displayed significant (61–63%) activity against *T. longifusus*, *A. flavus* and *C. glabrata* fungal strains, moderate (37–50%) activity against *C. albicans* and *M. canis*, and weaker (16%) activity against *F. solani*. Likewise, complex (**2**) had significant (55–77%) activity against *T. longifusus*, *A. flavus, M. canis*, and *C. glabrata*, and displayed weaker (25–26%) activity against remaining two strains. Similarly, the compound **3** demonstrated significant (55–69%) activity against *T. longifusus*, *A. flavus*, *M. canis*, and *C. glabrata*, moderate (42%) against *C. albicans* and weaker (23%) activity against *F. solani*. The complex (**4**) comparably possessed significant (55–65%) activity against *T. longifusus*, *A. flavus*, *M. canis*, and *C. glabrata* and moderate (36–37%) activity was observed with rest of the fungal strains. On the other hand, the compound (**5**)–(**8**) showed overall significant (55–75%) activity against all strains except *M. canis* which displayed weaker (17–30%) activity. The compounds (**9**)–(**16**) displayed overall significant (55–78%) activity against fungal strains due to Br and NO_2 groups attached with the aromatic rings. ($\mathbf{L^4}$) showed overall good fungal activity as compared to other three ligands due to nitro substitution. The Co(II) complex (**14**) of ($\mathbf{L^4}$) was found to be the most active complex. The metal (II)

Table 5. MIC (μg/mL) of the selected compounds (**9**), (**10**) and (**12**)–(**16**) against selected bacteria.

Compounds	*E. coli*	*S. flexneri*	*P. aeruginosa*	*S. typhi*	*S. aureus*
9	–	46.21	–	37.16	25.17
10	30.16	–	–	–	39.24
12	–	36.35	–	43.22	–
13	23.71	28.67	–	–	–
14	–	–	32.11	46.62	16.11
15	–	25.00	–	–	26.35
16	39.10	18.17	42.65	25.31	–

Table 4. Antifungal bioassay of ligands **($\mathbf{L^1}$)–($\mathbf{L^4}$)** and metal(II) complexes **(1)–(16)**.

	[% Inhibition (mm)]							
Compounds	(a)	(b)	(c)	(d)	(e)	(f)	(SA)	Average
$\mathbf{L^1}$	45	17	55	37	00	40	20.18	32.33
$\mathbf{L^2}$	38	56	49	00	43	30	19.77	36.00
$\mathbf{L^3}$	56	60	61	56	63	59	2.79	59.17
$\mathbf{L^4}$	62	58	59	63	61	55	2.94	59.67
1	62	37	63	49	16	61	18.63	48.00
2	55	25	75	77	26	58	22.81	52.67
3	59	42	62	55	23	69	16.66	51.67
4	65	36	64	56	37	57	12.91	52.50
5	57	68	66	17	75	66	20.97	58.17
6	61	69	72	28	69	71	16.94	61.67
7	55	73	67	30	66	75	16.72	61.00
8	56	64	68	25	68	69	17.03	58.33
9	71	75	70	67	72	74	2.88	71.50
10	75	69	57	73	70	67	6.32	68.50
11	69	74	70	65	69	65	3.39	68.67
12	70	78	68	74	73	60	6.19	70.50
13	72	75	70	61	72	64	5.37	69.00
14	78	65	57	73	70	67	7.20	68.33
15	69	58	70	65	72	65	5.01	66.50
16	75	68	72	77	79	68	4.62	73.17
SD	A	B	C	D	E	F	–	–

Average activity of ligands **($\mathbf{L^1}$)–($\mathbf{L^4}$)** = 46.79%; Average activity of complexes **(1)–(16)** = 62.51%; (a) *T. longifusus* (b) = *C. albicans* (c) = *A. flavus* (d) = *M. canis* (e) = *F. solani* (f) = *C. glabrata*; SD: standard drugs MIC μg/mL; A: Miconazole (70 μg/mL:1.6822 × 10^{-7} M/mL), B: Miconazole (110.8 μg/mL:2.6626 × 10^{-7} M/mL), C: Amphotericin B (20 μg/mL:2.1642 × 10^{-8} M/mL), D: Miconazole (98.4 μg/mL:2.3647 × 10^{-7} M/mL), E: Miconazole (73.25 μg/mL: 1.7603 × 10^{-7} M/mL), F: Miconazole (110.8 μg/mL: 2.66266 × 10^{-7} M/mL); weaker = 0–33%, moderate = 34–54%, 55–100% = significant; SA = statistical analysis.

Table 6. Cytotoxicity (*in vitro*) of ligands (**L^1**)–(**L^4**) and their metal(II) complexes **(1)–(16)**.

Compounds	LD_{50} (M/mL)	Compounds	LD_{50} (M/mL)	Compounds	LD_{50} (M/mL)
L^1	$>2.19 \times 10^{-3}$	**4**	$>1.64 \times 10^{-3}$	**11**	$>4.71 \times 10^{-3}$
L^2	$>1.81 \times 10^{-3}$	**5**	$>3.19 \times 10^{-3}$	**12**	$>2.68 \times 10^{-3}$
L^3	$>3.11 \times 10^{-3}$	**6**	$>4.04 \times 10^{-3}$	**13**	$>2.51 \times 10^{-3}$
L^4	$>2.19 \times 10^{-3}$	**7**	$>4.59 \times 10^{-4}$	**14**	$>2.11 \times 10^{-3}$
1	$>3.81 \times 10^{-3}$	**8**	$>2.81 \times 10^{-3}$	**15**	$>4.19 \times 10^{-4}$
2	$>2.11 \times 10^{-3}$	**9**	$>3.15 \times 10^{-3}$	**16**	$>3.81 \times 10^{-3}$
3	$>4.10 \times 10^{-3}$	**10**	$>1.98 \times 10^{-3}$		

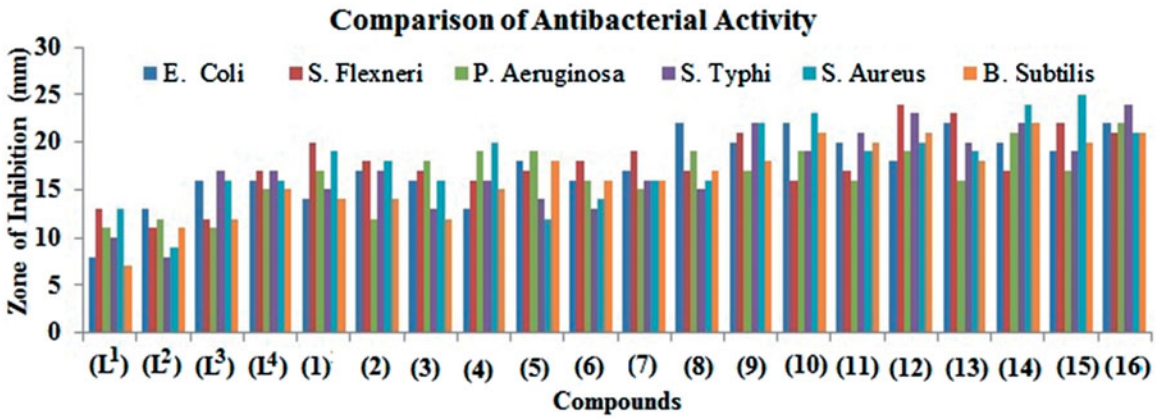

Figure 1. Comparison of antibacterial activity of Schiff's bases versus metal(II) complexes.

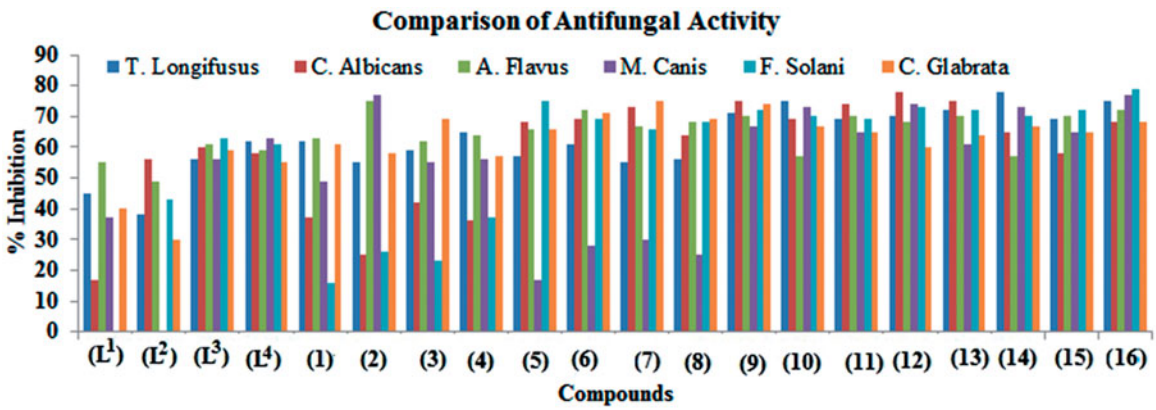

Figure 2. Comparison of antifungal activity of Schiff's bases versus metal(II) complexes.

complexes showed enhanced[31] activity results rather than their uncomplexed Schiff's bases upon complexation.

Minimum inhibitory concentration (MIC)

The synthesized ligands and their transition metal(II) complexes showing promising antibacterial activity (>80%) were selected for MIC studies i.e. the compounds (**9**), (**10**) and (**12**)–(**16**) and the results are reported in Table 5. The MIC values of these compounds fall in the range 23.11–46.62 g/mL. Among these, the compound (**14**) was found to be the most active possessing maximum inhibition of 16.11 μg/mL against the bacterial strain *S. Aureus*.

Cytotoxicity (in vitro)

The Schiff bases and their metal(II) complexes were screened for their cytotoxicity (brine shrimp bioassay) by using Meyer protocol[28]. The data recorded in Table 6 indicated that none of the compounds either ligands or complexes showed cytotoxicity (1.64×10^{-3} to 4.71×10^{-3}) against *Artemia salina*. The cytotoxic data recorded in Table 6 revealed that almost all compounds, ligands as well as metal complexes were inactive but it was interesting to note that the metal complexes displayed better potent cytotoxicity as compared to their parent ligands. This activity relationship may help to serve as a basis for future direction toward the development of certain cytotoxic agents for clinical applications.

Conclusions

The synthesized ethanol-derived Schiff's bases act as bi and tridentate ligands for coordination with the Co(II), Cu(II), Ni(II) and Zn(II) metal atoms. Physical (magnetic and molar conductance), spectral (IR, NMR, electronic) and analytical (C, H, N and metalloelements percentage) data confirmed that the Schiff base ligands are coordinated with the Co(II), Cu(II), Ni(II) and Zn(II)

metal atoms via azomethine-N, naphthalene-O, salicylidene-O and ethanol-O showing an octahedral geometry. The obtained results of antibacterial and antifungal activities indicated that the metal complexes possessed better biological activity against one or more bacterial and/or fungal strains as compared to their parent uncomplexed ligands. It can be asserted that azomethine-N, nitro, bromo and oxygen were the functional groups in the compounds potentially responsible for the enhancement of bacterial and fungal activities. However, brine shrimp assays revealed that these compounds were limited in their cytotoxicity hinting at some divergent apoptotic mechanisms.

Acknowledgements

The authors are grateful to HEJ research Institute of Chemistry, University of Karachi, Pakistan, for providing their help in taking NMR, mass spectra and for the help in carrying out antibacterial, antifungal and brine shrimp bioassays.

Declaration of interest

The authors declare no conflict of interest.

References

1. Schiff H. Mittheilungen aus dem Universitätslaboratorium in Pisa: Eine neue Reihe organischer Basen. Justus Liebigs Annalen Der Chemie 1864;131:118–19.
2. Das P, Linert W. Schiff base-derived homogeneous and heterogeneous palladium catalysts for the Suzuki–Miyaura reaction. Coordination Chem Rev 2016 15;311:1–23.
3. Chohan ZH, Hanif M. Synthesis and characterization of biologically active new Schiff bases containing 3-functionalized 1,2,4-triazoles and their zinc(II) complexes: crystal structure of 4-bromo-2-[(*E*)-(1H-1,2,4-triazol-3-ylimino)-methyl]phenol. Appl Organomet Chem 2011;25:753–60.
4. Haasnoot JG. Mononuclear, oligonuclear and polynuclear metal coordination compounds with 1, 2, 4-triazole derivatives as ligands. Coord Chem Rev 2000;200–202:131–85.
5. Chohan ZH, Hanif M. Design, synthesis, and biological properties of triazole derived compounds and their transition metal complexes. J Enzyme Inhib Med Chem 2010;25:737–49.
6. Holla BS, Veerendra B, Shivanada MK, Poojary B. Synthesis, characterization and anticancer activity studies on some Mannich bases derived from 1,2,4-triazoles. Eur J Med Chem 2003;38: 759–67.
7. Arion VB, Reisner E, Fremuth, et al. Synthesis, X-ray diffraction structures, spectroscopic properties, and in vitro antitumor activity of isomeric (1*H*-1,2,4-triazole)Ru(III) complexes. Inorg Chem 2003; 4:6024–31.
8. Habtemariam A, Melchart M, Fernández R, et al. Structure-activity relationships for cytotoxic ruthenium (II) arene complexes containing N, N-, N, O-, and O, O-chelating ligands. J Med Chem 2006;49: 6858–68.
9. Hussein MA, Shaker RM, Ameen MA, Mohammed MF. Synthesis, anti-inflammatory, analgesic, and antibacterial activities of some triazole, triazolothiadiazole, and triazolothiadiazine derivatives. Arch Pharm Res 2011;34:1239–50.
10. Cui XS, Jing C, Chai KY, et al. Synthesis and anticonvulsant evaluation of 3-substituted-4-(4-hexyloxyphenyl)-4H-1,2,4-triazoles. Med Chem Res 2009;18:49–58.
11. Kritsanida M, Mouroutsou A, Marakos P, et al. Synthesis and antiviral activity evaluation of some new 6-substituted 3-(1-adamantyl)-1,2,4-triazolo[3,4-b][1,3,4]thiadiazoles. IlFarmaco 2002;57:253–7.
12. Turan-Zitouni G, Kaplancikli ZA, Erol K, Kilic FS. Synthesis and analgesic activity of some triazoles and triazolothiadiazines. Farmaco 1999;54:218–23.
13. Karaoglu K, Baran T, Degirmencioglu I, Serbest K. Synthesis and spectroscopic studies of homo-binuclear, alkoxo bridged homo-and hetero tetranuclear metal complexes of a bis N_2O_4 Schiff base ligand derived from ethanolamine and macroacyclic tetra naphthaldehyde. Spectrochi Acta A: Mol Biomol Spectr 2011;79:862–72.
14. Masoud MS, El-Einein SAA, Abed IM, Ali AE. Synthesis and characterization of amino alcohol complexes. J Cood Chem 2002; 55:153–78.
15. Carrasco F. Ingredientes Cosméticos. Diccionario de Ingredientes Cosméticos. 4th ed. Malaga, Spain; 2009:306.
16. Salem IA. Role of resin-manganese(II) complexes in hydrogen peroxide decomposition. Int J Chem Kin 1994;26:341–6.
17. Weissermel K, Arpe HJ. Chap. 7. Oxidation products of ethylene. In: Industrial organic chemistry. Weinheim, Germany: Wiley-VCH; 2003:159–61.
18. Jakubovic AO. Anion exchangers from the reaction of cellulose with amines and epichlorhydrin. Polymer Sci 1960;117–19.
19. Elsayed AH, Haffz AM. Study of dielectric relaxation in Zn, Cd, and Hg, ethanolamine complexes. Egy J Sol 2005;28:53.
20. Flores-Parra A, Contreros R. Boron coordination compounds derived from organic molecule of biological interest. Coord Chem Rev 2000;196:85–124.
21. Han L, Gao JR, Li ZM Z, et al. Synthesis of new plant growth regulator: N-(fatty acid) O-aryloxyacetyl ethanolamine. Bioorg Med Chem Lett 2007;17:3231–4.
22. Chohan ZH, Naseer MM. Organometallic based biologically active compounds: synthesis of mono- and di-ethanolamine derived ferrocenes with antibacterial, antifungal and cytotoxic properties. App Organomet Chem 2007;21:1005–12.
23. Akram MS, Rehman JU, Hall EA. Engineered proteins for bioelectrochemistry. Annu Rev Anal Chem 2014;7:257–74.
24. Clarke RM, Storr T. The chemistry and applications of multimetallic salen complexes. Dalton Trans 2014;43:9380–91.
25. Syaxal A, Singhal O.P, Banerjee S. Synthesis of new dioxouranium(VI) complexes with tridentate diabasic schiff bases derived from salicylaldehyde or substituted salicylaldehyde and ethanolamine. Synth React Inorg Metal-Org Chem 1980;10:243–53.
26. Rahman AU, Choudhary MI, Thomsen WJ. Bioassay techniques for drug development. The Netherlands: Harwood Academic Publishers; 2001.
27. McLaughlin JL, Chang CJ, Smith DL. Studies in natural products chemistry, 'Bentch-Top'. In: Atta-ur-Rahman, ed. Bioassays for the discovery of bioactive natural products: an update, structure and chemistry (part-B). Vol. 9. The Netherlands: Elsevier Science Publishers; 1991:383.
28. Meyer BN, Ferrigni NR, Putnam JE, et al. Brine shrimp: a convenient general bioassay for active plant constituents. Planta Med 1982;45:31–4.
29. Finney DJ. Probit analysis. 3rd ed. Cambridge, MA: Cambridge University Press; 1971.
30. Holla BS, Mahalinga M, Karthikeyan MS, et al. Synthesis, characterization and antimicrobial activity of some substituted 1,2,3-triazoles. Eur J Med Chem 2005;40:1173–8.
31. Sumrra SH, Chohan ZH. In vitro antibacterial, antifungal and cytotoxic activities of some triazole schiff bases and their oxovanadium(IV) complexes. J Enzyme Inhib Med Chem 2013;28: 1291–9.
32. Hanif M, Chohan ZH. Design, spectral characterization and biological studies of transition metal(II) complexes with triazole schiff bases. Spectrochim Acta A Mol Biomol Spectrosc 2013;104: 468–76.
33. Nakamoto K. Infrared spectra of inorganic and coordination compounds. 2nd ed. NewYork: Wiley Interscience; 1970.
34. Sumrra SH, Chohan ZH. Metal based new triazoles: their synthesis, characterization and antibacterial/antifungal activities. Spectrochim Acta Part A: Mol Biomol Spectr 2012;98:53–61.
35. Ferrero JR. Low-frequency vibrations of inorganic and coordination compounds. New York: John Wiley; 1971.
36. Nyquist RA. Interpreting Infrared, Raman, and Nuclear Magnetic Resonance Spectra. Orlando: Academic Press; 2001:2.
37. Freeman RA. Handbook of nuclear magnetic resonance. 2nd ed. London, UK: Longman Publishing, 1997.
38. Geary WJ. The use of conductivity measurements in organic solvents for the characterisation of coordination compounds. Coord Chem Rev 1971;7:81.
39. Balhausen CJ. An introduction to ligand field theory. New York: McGraw Hill; 1962.
40. Lever ABP. Inorganic electronic spectroscopy. New York: Elsevier; 1984.
41. Nair MS, Joseyphus RS. Synthesis and characterization of Co(II), Ni(II), Cu(II) and Zn(II) complexes of tridentate Schiff base derived

from vanillin and DL-alpha-aminobutyric acid. Spectrochim Acta A Mol Biomol Spectrosc 2008;70:749–53.
42. Chohan ZH, Shaikh AU, Supuran CT. In-vitro antibacterial, antifungal and cytotoxic activity of cobalt (II), copper (II), nickel (II) and zinc (II) complexes with furanyl methyl- and thienyl methyl-dithiolenes: 1,3-dithiole-2-one and 1,3-dithiole-2-thione. J Enzyme Inhib Med Chem 2006;21:733–40.
43. Kaushal R, Thakur S. Syntheses and biological screening of Schiff base complexes of titanium(IV). Chem Eng Trans 2013;32:1801–6.
44. Ejidike IP, Ajibade PA. Synthesis, characterization, antioxidant, and antibacterial studies of some metal(II) complexes of tetradentate schiff base ligand: (4E)-4-[(2-{(E)-[1-(2,4-dihydroxyphenyl)ethylidene]amino}ethyl)imino]pentan-2-one. Bioinorg Chem Appl 2015; 2015:890734.
45. Larabi L, Hared Y, Reguig A, Mostafa M. Synthesis, structural study and electrochemical properties of copper (II) complexes derived from benzene and p-toluenesulphonylhydrazone. J Serb Chem Soc 2003;68:85–95.
46. Badawy MA, Mohamed GG, Omar MM, et al. Synthesis, spectroscopic and thermal characterization of quinoxaline metal complexes. Eur J Chem 2010;1:282–8.
47. Rehman SU, Chohan ZH, Naz F, Supuran CT. In-vitro antibacterial, antifungal and cytotoxic activities of some coumarins and their metal complexes. J Enzyme Inhib Med Chem 2005;20:333–40.
48. Sumrra SH, Chohan ZH. Synthesis, characterization and biological properties of thienyl derived triazole Schiff bases and their oxovanadium(IV) complexes. J Enzyme Inhib Med Chem 2012;27: 187–93.